Available online at www.sciencedirect.com
ScienceDirect
C. R. Physique ••• (••••) •••–•••
COMPTES RENDUS PHYSIQUE
http://france.elsevier.com/direct/COMREN/

Theoretical spectroscopy / Spectroscopie théorique

# The challenge of predicting optical properties of biomolecules: what can we learn from time-dependent density-functional theory?

Alberto Castro [a,b], Miguel A.L. Marques [c,d,b], Daniele Varsano [e,b], Francesco Sottile [f,b], Angel Rubio [g,h,b,*]

[a] *Institut für Theoretische Physik, Fachbereich Physik, Freie Universität Berlin, 14195 Berlin, Germany*
[b] *European Theoretical Spectroscopy Facility (ETSF)*
[c] *Laboratoire de physique de la matière condensée et nanostructures, Université Lyon I, CNRS, UMR 5586, domaine scientifique de la Doua, 69622 Villeurbanne cedex, France*
[d] *Centre for Computational Physics, Department of Physics, University of Coimbra, 3004-516 Coimbra, Portugal*
[e] *National Center on nanoStructures and bioSystems at Surfaces (S3) of INFM-CNR, c/o Dipartimento di Fisica, Università di Modena e Reggio Emilia, Via Campi 213/A, 41100 Modena, Italy*
[f] *Laboratoire des solides irradies, École polytechnique, 91128 Palaiseau cedex, France*
[g] *Departamento de Fisica de Materiales, Universidad del País Vasco, Edificio Korta, 20018 San Sebastián, Spain*
[h] *Centro Mixto CSIC-UPV/EHU and DIPC, Universidad del País Vasco, 20018 San Sebastián, Spain*

**Abstract**

The suitability of the time-dependent density-functional theory (TDDFT) approach for the theoretical study of the optical properties of biomolecules is demonstrated by several examples. We critically discuss the limitations of available TDDFT implementations to address some of the present open questions in the description of the excited-state dynamics of biological complexes. The key objective of the present work is to address the performance of TDDFT in the linear response regime of the bio-molecular systems to the visible or near UV radiation – measured by, e.g. optical absorption or optical dichroism spectra. Although these spectra are essentially determined by the electronic degrees of freedom of small, optically active regions within the usually large biological systems, they can also be strongly influenced by environment effects (solvent, hosting protein, temperature, etc.). Moreover, many key biological processes consist of photo-induced dynamics (photoisomerisation, etc.), and their description requires a coupled treatment of electronic and nuclear degrees of freedom. We illustrate these aspects with a selection of paradigmatic biomolecular systems: chromophores in fluorescent proteins, porphyrins, DNA basis, the azobenzene dye, etc. ***To cite this article: A. Castro et al., C. R. Physique ••• (••••).***


**Résumé**

**Le défi de la prédiction des propriétés optiques des bio-molécules : que peut nous apprendre la théorie de la fonctionnelle de la densité dépendante du temps ?** L'utilité de la théorie de la fonctionnelle de la densité dépendante du temps (TDDFT) pour l'étude théorique des propriétés optiques de biomolécules a été largement démontrée. Nous discutons les limites des implémentations actuelles de la TDDFT, afin de répondre à certaines questions sur la description des états excités des systèmes biologiques complexes. L'objectif principal de ce travail est d'évaluer les performances de la TDDFT, en régime linéaire, pour les systèmes bio-moléculaires, dans le spectre visible ou UV proche – mesuré, par exemple, avec l'absorption optique ou le dichroïsme optique.

* Corresponding author at: Departamento de Fisica de Materiales, Universidad del País Vasco, Edificio Korta, 20018 San Sebastián, Spain.
*E-mail address:* angel.rubio@ehu.es (A. Rubio).

1631-0705/$ – see front matter © 2008 Published by Elsevier Masson SAS on behalf of Académie des sciences.
doi:10.1016/j.crhy.2008.09.001

Bien que ces spectres soient essentiellement déterminés par les degrées de liberté électroniques, les régions optiquement actives des grands systèmes biologiques peuvent être fortement influencés par les effets dus à l'environnement (solvant, entourage de la protéine, température, etc.). De plus, de nombreux processus biologiques essentiels sont des processus dynamiques photo-induits (photoisomérisation, etc.), et leur description a besoin d'un traitement conjoint des degrés de liberté électroniques et nucléaires. Nous illustrons ces aspects avec une sélection de systèmes bio-moléculaires paradigmatiques : chromophores des protéines fluorescentes, porphyrines, ADN, azobenzène, etc. ***Pour citer cet article : A. Castro et al., C. R. Physique ••• (••••).***


*Keywords:* Biomolecules; Excitations; TDDFT

*Mots-clés :* Biomolécules ; Excitations ; TDDFT

## 1. Introduction

Absorption or emission of light from biomolecules are crucial processes to understand the machinery of life [1]. Photosynthesis [2], vision [3], bioluminescence [4] or DNA damage are paradigmatic examples. A sound theoretical understanding of the photo-chemistry of biological molecules is not only needed to describe the mechanisms of Biology, but also because some of the key molecules can be employed for technological purposes at the nanoscale [5]. However, despite the tremendous effort focused on this field, the first-principles theoretical description of the interaction of these molecules with time-dependent electromagnetic fields is still a challenging problem, lacking a definitive and systematic methodology, capable of bridging the different spatial and time scales that are relevant for the description of light-induced biological processes with predictive power.

Time-dependent density-functional theory (TDDFT) [6] has repeatedly shown in the last decade its usefulness when attempting this challenge. The reason is the unparallelled balance between the computational load that it requires and the accuracy that it provides. In the past few years, we have performed a number of theoretical studies on the photo-response of organic and biological molecules by making use of TDDFT. It is the purpose of this article to overview, by showing several of these examples, some of the capabilities of this approach and highlight the deficiencies of present approximations for the unknown frequency-dependent exchange-correlation kernel that enters the TDDFT equations.

The visible and near ultraviolet (UV) range of the spectrum is, of course, specially relevant – and it is indeed the visible and UV spectroscopy the main applicability niche of TDDFT. We will therefore concentrate on this area. Most organic molecules, however, are completely transparent to visible light, and begin to absorb in the UV region. Upon absorption of a photon, a molecule undergoes a transition between two molecular states. The most common transitions are of the $\sigma$ to $\sigma^*$, $\pi$ to $\pi^*$ and $\pi$ to $n\pi$ kind, and correspond to absorption of light in the UV. In molecular chains with alternate bonds, however, absorption can be shifted to longer wavelengths. In these so-called conjugated molecules, electrons are delocalised over the whole system. Therefore, by increasing the length of the molecule, $\pi$-electrons become more delocalised, and the HOMO-LUMO energy gap decreases. If the system is long enough, optical absorption may lie in the visible region. Chromophores are those organic molecules with long conjugated bonds, resulting in very efficient absorption in the visible or near-UV regions of the spectrum. Sections 2 and 3 are dedicated to some examples of this large family of molecules.

Section 4 is dedicated to the optical properties of DNA basis and compounds. TDDFT may help in this case to analyse how the response of the nucleobases is altered by their mutual interaction, either in their natural environment (where the bases are paired in the Watson–Crick (WC) scheme, and covalently bound to a sugar-phosphate backbone), or in synthesised arrangements. The favourable scaling properties of TDDFT with respect to traditional Quantum Chemistry approaches is in this case crucial to be able to study the evolution of excited state properties as the size of the DNA compounds grows. We also show calculations of the circular dichroism of the adenine molecule and dimer, where it is highlighted the relevance of the circular dichroism spectra to address the properties of stacked bases (including the chirality of molecules).

TDDFT, in principle, addresses the electronic problem of a molecular system; the study of the nuclear movement requires some form of molecular dynamics. Section 5 is dedicated to some approaches to this coupling between TDDFT and molecular dynamics. The systems chosen for this purpose are the azobenzene chromophore (whose fast isomerisation has a large potential for technological applications), and formaldimine, which also illustrates the double-bond rotation that underlies many biological dynamical processes. As a somehow exotic excursion, Subsection 5.3

Please cite this article in press as: A. Castro et al., The challenge of predicting optical properties of biomolecules: what can we learn from time-dependent density-functional theory?, C. R. Physique (2008), doi:10.1016/j.crhy.2008.09.001

displays a particularly intuitive way of monitoring the chemical bonds during a dynamical molecular process: the time-dependent electron-localisation function (TDELF), which can be effectively extracted from a TDDFT calculation.

Most of the calculations reported in this Article have been performed with our own TDDFT implementation, the `octopus` code. We refer the reader to Refs. [7] and [8] for technical details regarding the algorithms. Moreover, we focus here on the results of the applications, rather than on the description of the theory itself. References [6,9–12] are some possibles sources to get acquainted with the foundations of TDDFT.

## 2. Chromophores in proteins

Biochromophores are never isolated in nature, but are typically covalently bound to a protein. For instance, retinol, present in our eyes and responsible for capturing the photons in the first stage of the vision process, is always a part of some protein – of any in the so called "opsin" family. The proteic surroundings may have a strong influence on the response of a chromophore to light. Following with the retinol example, the absorption maximum of the chromophore in the protein red-shifts by about 120 nm with respect to the chromophore in solution. It is clear that any successful theoretical treatment of the optical response of a chromophore must include consistently the effect of its environment.

The photoactive region, however, is usually constituted by a relatively small active centre – the chromophore, and the surrounding medium – and the rest of the molecule plus the environment can be considered as a perturbation. The environment can be a solution, or even a solid-state device. Optical processes related, for instance, to vision and photosynthesis, rely on a subtle interplay between optical absorption by the photoactive centre and its decay mechanism through the coupling to the internal vibrational modes of the molecule, including isomerisation processes, as well as the coupling to the environment (the supporting protein and the solvent). In the following, we supply some recent examples of application of TDDFT to the calculation of absorption spectra of biomolecules, namely of the so called fluorescent proteins. These constitute a set of molecules with a wide range of applications as biological markers [13] – and now are also being used to form hybrid devices for nano-optic applications [14].

### *2.1. The green fluorescent protein (GFP)*

A complex and appealing photoactive molecule is the green flourescent protein (GFP). This molecule has been studied experimentally in various environments, in solution as well as *in vacuo*, and has been found to exhibit a rich and complex behaviour that is the subject of much current debate. The measured optical absorption spectrum of the wild type (wt) GFP shows two main resonances at 2.63 and 3.05 eV [15,16] (see Fig. 1), that are attributed to two different thermodynamically stable protonation states of the chromophore, the neutral and the negative configurations of the chromophore, respectively. So far, ab-initio quantum chemistry has not been able to provide satisfactory agreement with the spectroscopic data, and has not contributed much to confirm or rule out various possible scenarios of photo-dynamics in the GFP. A good description of the optical properties of the GFP photoreceptor has been achieved [17] by using an approach that combines (a) a hybrid quantum mechanics-molecular mechanics (QM-MM) method to obtain the structure, with (b) time-dependent density functional theory to treat the electronic excitations.

The structures were first optimised using a QM-MM method [18–20] with a semiempirical Hamiltonian [21] to describe the quantum subsystem. The quantum mechanical (QM) region included a sequence of three amino-acids that form the chromophore: Ser65, Tyr66 and Gly67. The optimised structure of the chromophore, with the most important neighbour residues, is shown in Fig. 1. On the other hand, the anionic form of the chromophore was obtained by deprotonation of Tyr66 and protonation of Glu222. The calculated photoabsorption spectra of the GFP neutral and anionic chromophores, shown also in Fig. 1, are in excellent agreement with experiment assuming the presence of the two forms of the photo-receptor, protonated and deprotonated respectively, in an approximate 4:1 ratio. Furthermore, it can be seen in the inset of Fig. 1 that light polarised along the $x$-direction is responsible for the lowest optical transition in the neutral chromophore. The molecule is nearly transparent to visible light polarised along the other two orthogonal directions. The GFP turns out to be a rather anisotropic molecule in the visible region, a property that could be used to enhance the photo-dynamical processes in well oriented GFP samples for opto-electronic devices. It should be emphasised that good agreement is obtained because the breaking of the planarity of the biochromopeptide caused by the protein surrounding has been taken into account. Notice also that the measured peaks can be clearly assigned to either the neutral or anionic forms of the GFP.

Please cite this article in press as: A. Castro et al., The challenge of predicting optical properties of biomolecules: what can we learn from time-dependent density-functional theory?, C. R. Physique (2008), doi:10.1016/j.crhy.2008.09.001

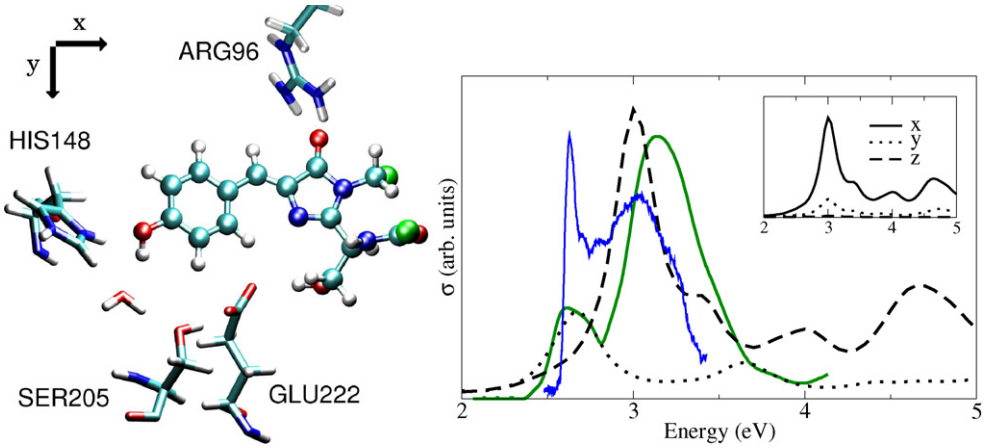


Fig. 1. Left panel: Optimised structure of the neutral chromophore and its closest charged residues inside the green fluorescent protein (GFP): His148, Arg96 (positive) and Glu222 (negative). Right panel: Computed photoabsorption cross section of the neutral (dashed line) and anionic (dotted line) chromophores. For comparative purposes the anionic results have been divided by 4. Experimental results at 1.6 K (blue) [15] and room temperature (green) [16] are also given. The insert gives a decomposition of the calculated spectrum of the neutral chromophore in the three directions, showing the inherent anisotropy of the GPF molecule.

### 2.2. *The blue mutant of the GFP*

In the past years there has been an increasing demand for the ability to visualise different proteins in vivo that require multicolour mode imaging. For this reason, several groups set forth to develop GFP-mutant forms with different optical responses. A mutant of the GFP of particular interest is the Y66H variant, in which the aminoacid Tyr66 of the GFP is mutated to a Histidine [22,23]. The resultant protein exhibits fluorescence shifted to the blue range, and is for that reason often referred to as the blue emission variant of the GFP, or the blue fluorescent protein (BFP). The BFP chromophore is considerably more complicated than the GFP. It has four possible protonation states: one anionic (named HSA), two neutral (HSD and HSE), and one cationic (HSP). Each one of them, in turn, has two possible stable conformations, one cis and one trans, joined by a transition state. The optical spectra of all these configurations, as obtained by means of TDLDA, is shown in Fig. 2.

The main candidate to explain the experimental spectrum of the BFP turns out to be a neutral-cis configuration. However, in contrast to the wt-GFP where the response of the anionic and of neutral states occurs at distinct frequency ranges [24–26], in the BFP both anionic and neutral configurations have very similar spectra, with only minor differences in the fine structure close to the main peak. On the other hand, even if the absorption spectrum is not conclusive, the acid dissociation constant ($pK_a$) analysis seems to rule out the existence of the anionic state in vivo. Furthermore, other protonation states (such as the cationic) cannot be present in the BFP protein as their spectral features are outside the measured absorption spectra.

Like in the GFP, it is quite important to take into account the role of the chromophore environment. This role is 2-fold: (i) it induces structural modifications of the gas phase chromophore, the most important being the breaking of the planarity of the imida rings; and (ii) it makes a local-field modification of the external electromagnetic field. To study these effects, QM/MM simulations of the chromopeptide embedded inside the BFP were performed (see Ref. [26] for computational details). We will discuss here the cis-HSD case, since it is the lowest energy structure for the neutral chromophore, and X-ray data indicate a cis conformation, therefore making it the most likely candidate to be present in the experiments.

Regarding the structure, the protein induces the breaking of planarity (around 18°) of the otherwise planar gas-phase structure. Then, in order to determine the role played by the protein intra-media in the optical spectroscopy properties of the chromopeptide, the authors selected several structures from the QM/MM minimisation and performed TDDFT calculations. These calculations are summarised in Fig. 3, along with the calculated gas phase result (named "Gas-phase" in the figure), and the experimental spectrum. The spectrum of the bare chromophore, but as distorted by the protein environment, is denoted "Distorted". The other two curves correspond to the chromopeptide plus a selection of some the closest residues (the *environment*): "Env I" includes His148, Glu222, and Arg96, which are

Please cite this article in press as: A. Castro et al., The challenge of predicting optical properties of biomolecules: what can we learn from time-dependent density-functional theory?, C. R. Physique (2008), doi:10.1016/j.crhy.2008.09.001

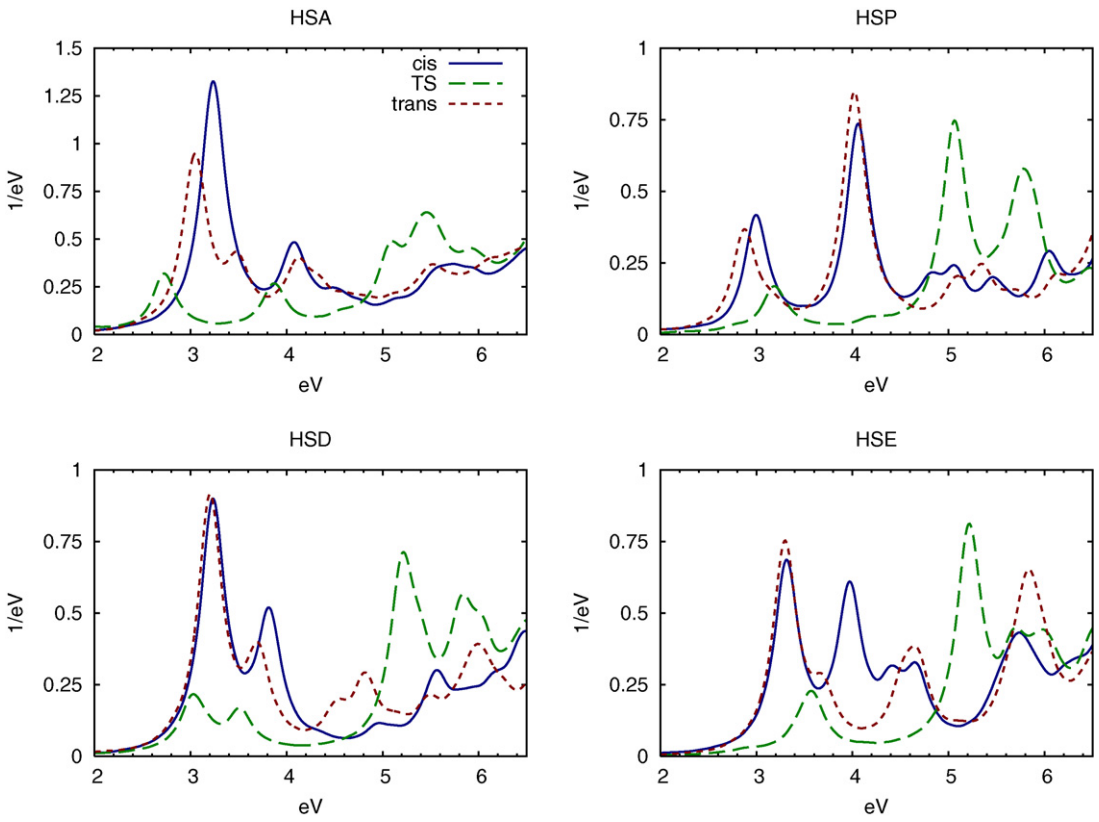


Fig. 2. Calculated TDLDA optical absorption spectrum in the range 2–5 eV for the various protonation states and conformers of the chromopeptide in the gas phase (cis: solid line; TS: dashed line; and trans: dotted line).

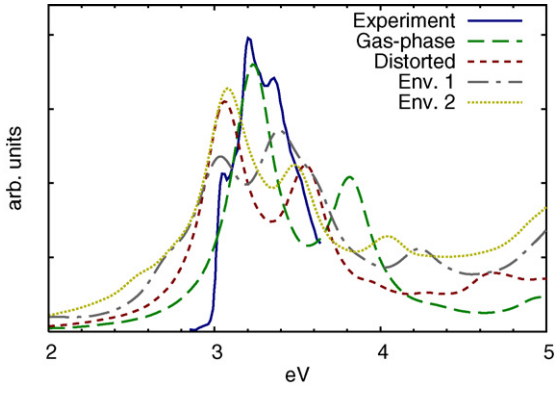


Fig. 3. Calculated TDLDA optical absorption spectrum for the cis-HSD state of the chromophore in the gas phase and distorted by the BFP protein environment, compared with the experimental spectrum of the BFP.

the charged residues in the vicinity of the chromophore (His148 and Arg96 positive; Glu222 negative). As such, it is reasonable to expect that they will have a greater influence in polarising the electronic cloud of the chromopeptide. "Env II" is made of "Env. II" plus Ser205, a buried water molecule, and Gln94. All of these are polar residues that are within 2.5 Å of the chromophore.

It can be seen how the induced non-planarity has a sizable effect in the spectrum. It causes a considerable red-shift of the gas-phase cis-HSD peaks. Thus, the optical spectrum is sensitive to the $\approx 20^\circ$ torsion. On the other hand, the effect of the polarisation of the electronic cloud by neighbour residues is less important. The inclusion of the residues

Please cite this article in press as: A. Castro et al., The challenge of predicting optical properties of biomolecules: what can we learn from time-dependent density-functional theory?, C. R. Physique (2008), doi:10.1016/j.crhy.2008.09.001

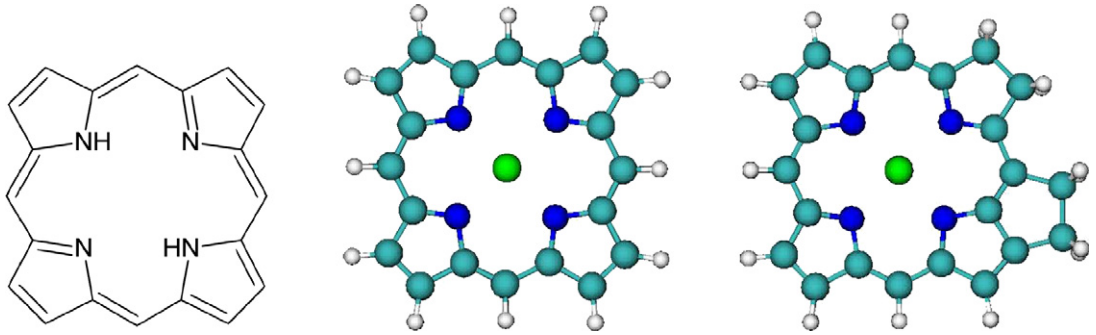


Fig. 4. Left: basic porphyrine structure. Centre and right: symmetric and asymmetric Magnesium porphyrine-like molecules (the asymmetry was introduced by closing a pentagonal ring close to the bottom right amida ring).

in "Env I" in the TDLDA calculation causes a further red-shift of the second peak, but leaves the first peak almost unchanged. However, when enlarging the environment to "Env II", we find a spectrum with a shape similar to the one of the twisted chromopeptide with two well-defined peaks at similar positions. It seems that "Env I" provides an inhomogeneous surrounding, which leads to an over-polarisation, and this artifact is corrected by the inclusion of a larger environment.

In summary, the optical absorption inside the BFP exhibits a red shift of about 0.15 eV, which has mainly a structural origin – a breakdown of planarity. This could be responsible for the 0.13 eV red-shift observed between folded and unfolded conformations of the BFP protein [22]. Furthermore, there is a subtle cancellation between the shielding of the electromagnetic field acting on the chromophore due to its closest residues. This cancellation effect makes that the calculated spectra for the isolated (twisted) chromophore and for the chromophore in the protein are nearly identical. Another aspect that we have shown to be relevant is the inclusion of temperature [26] that is important to bring more quantitative agreement between the calculated BFP spectra and the measured one. Temperature introduces fluctuations in the dihedral angle related to the breaking of planarity in the BFP chromophore (floppy torsional motion of the two imida-rings are included), and consequently to a broadening and shift of the calculated spectra. We note this breaking of planarity plays a fundamental role in the description of the optical properties of other GFP-mutants also studied by our group [27].

## 3. Porphyrins

The porphyrin family [28] is perhaps the paradigm of coloured organic molecules existing in nature ("porphura" meaning "purple pigment" in Greek). The basic constituent of all the members of the family is the porphyne; it consists of four pyrrole units linked by four methine bridges (see Fig. 4). It is an aromatic molecule containing 22 $\pi$ electrons – which is already an indication of its potential to be active in the visible range of the spectrum. Substitutions and small modifications of this basic structure produce the porphyrin molecules. Usually, a metal is inserted in the canter of the molecule; for example, if it is iron, the porphyrins are called "hemes"; the well known hemoglobin is a protein whose active canter is a heme group (an *hemoprotein*). There is a vast range of different natural and man-made metallo-porphyrin based compounds that evidence the huge field of research that this set of molecules form.

Chlorins are "almost" porphyrins and we can consider them members of this family: the only defining difference is that one of the four pyrroles is reduced and therefore the structure is not aromatic across the full molecular ring. If the chlorin hosts one magnesium atom at its centre, then it constitutes the basic tetrapyrrole of chlorophyll, the well known light harvester present in most plants and algae. This molecule has a characteristic absorption pattern in the visible range of the spectrum: strongly in the red and blue areas, weakly in the green.

More than 50 different types of chlorophylls have been found in living photosynthetic organisms. There exists, in fact, a large variety of additional structural elements to the tetrapyrrole, all giving rise to different vis-UV spectra, one of the most characteristic (important for both structural and electronic properties) being the pythol chain, that normally anchors the pigment to the protein structure.

Since the chlorophylls are derivatives of the porphyrin family, the main features of their optical properties can be understood, from a theoretical point of view, from a study of the latter. However, as we show in Fig. 5, the plain,

Please cite this article in press as: A. Castro et al., The challenge of predicting optical properties of biomolecules: what can we learn from time-dependent density-functional theory?, C. R. Physique (2008), doi:10.1016/j.crhy.2008.09.001

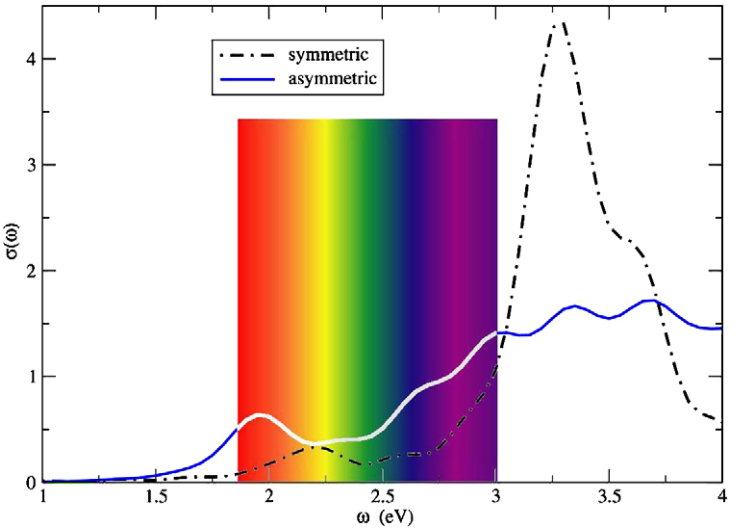


Fig. 5. Calculated TDLDA photoabsorption spectrum of the symmetric and asymmetric forms of the Mg-porphyrin depicted in Fig. 4 (see text for details). The visible part of the spectrum is highlighted as a guide for the eye.

symmetric, flat Mg porphyrin (Fig. 4, centre) cannot on its own give rise to the double-peak absorption typical of chlorophylls. In fact, the smallest representative of chlorophyll is not the plain, symmetric porphyrin structure presented in the left, but the more asymmetric one presented on the right (Fig. 4), and characterised by a fifth isocyclic ring. In this 5-ring porphyrin, the pyrrole ring IV is saturated and as a consequence some transitions shift towards the red and gain oscillator strength. The more asymmetric the $\pi$-electron distribution is, the more emphasised the double-peak shape will be (the structure at the centre of Fig. 4 is too symmetric, leading to HOMO's degeneracy, and is then not capable to reproduce the richer chlorophyll spectrum shape). Other details of the chlorophyll structure, like bending, protonation, addition and/or distortion of other elements, might further shift and vary the optical peaks: still the most significant effect stems from the breaking of the square symmetry of the basic porphyrine structure. These ab initio results support the simple exciton-model (4-band model [29]) that has been used in the last two decades to describe experimental results and, at the same time, underline the pertinence and the usefulness of TDDFT, already at the very basic approximations (here LDA/GGA), for a global understanding of the process of light absorption. Still, in the photosynthetic units, besides the absorption process, the conversion of energy also depends on charge-transfer excitation mechanisms that are poorly described by present LDA/GGA functionals (see Section 6 below). On the other hand, the promising results found in this sections open the way towards the description of hybrid devices made of porphyrins and nanowires for either photovoltaic-energy conversion and/or volatile memory devices [30].

## 4. Optical response of DNA bases and base pairs

In order to characterise either the structural or the response properties of biomolecular systems, it is crucial to be able to distinguish the intrinsic molecular properties from the effects induced by the environment (e.g. the solvent). The optical absorption spectrum may be able to properly discriminate those effects, hence its success as a characterisation tool. This fact is specially important for DNA and DNA-based compounds [32,33].

In addition to the obvious relevance of scientific investigations of DNA molecules for medical and biological purposes, we have witnessed lately how DNA compounds and DNA-like derivatives, are studied for their potential applications for nanotechnological purposes. The reasons are its stability (in solution), its one-dimensional character, along with the unique properties of self-assembly and recognition. However, in order to advance farther this technological line of research, the determination and interpretation of the electronic properties of nucleobases and of DNA helical arrangements is an extremely valuable foreword, and notable multidisciplinary efforts are currently devoted to such goals [34–39]. Furthermore, knowledge of the electronic properties, excited-state lifetimes, and ultraviolet (UV) absorption spectra is of paramount importance for our understanding of, e.g., the crucial phenomenon of UV radiation-induced DNA damage.

Please cite this article in press as: A. Castro et al., The challenge of predicting optical properties of biomolecules: what can we learn from time-dependent density-functional theory?, C. R. Physique (2008), doi:10.1016/j.crhy.2008.09.001

To relate the optical properties of nucleic acids to their structure, spatial conformation, and type of intra-molecular interactions, a valuable preliminary step is to gain insight into the excited-state properties of their building blocks, namely the monomeric bases, and to understand the role of hydrogen-bonding and stacking when these monomeric units form complex assemblies. In their natural environment, the DNA bases are paired via hydrogen-bonds in the WC scheme [44], and are covalently bonded to the sugar-phosphate backbone. The hydrogen-bonded base pairs interact with each other in the typical helical arrangement by inter-plane Van der Waals forces. To disentangle how the different interactions control the DNA dynamics upon light absorption, it is important to infer how the spectrum of a given isolated nucleobase is modified by mutual interactions in the different spatial conformations of DNA assemblies. TDDFT certainly is an appropriate tool for attempting this task.

In Ref. [31] a complete study of the optical absorption spectra of the five isolated gas-phase nucleobases and some of their assemblies is reported: simple WC pairs, simple $\pi$-stacks of two bases and more complex $\pi$-stacks of WC guanine–cytosine (GC) pairs. These calculations of isolated simple nucleobase-assemblies are a remarkable playground to prove the reliability of TDDFT for DNA-based materials. For the first time, the optical properties for a helical conformation of two stacked GC pairs [d(GC)] were computed by an ab-initio method. For such a conformation, H-bonding (which leads to the formation of WC pairs) and $\pi$-stacking effects are active simultaneously and can be distinguished.

The results discussed below and in Ref. [31] can be summarised as follows. For the isolated bases we obtained absorption spectra in rather good agreement with previous theoretical works and (qualitatively) with experiments (see Tables 1 to 6 of Ref. [31] for a detailed comparison between TDDFT excitation energies and experiments, and Tables 4 to 6 of Ref. [33] for comparison with quantum chemical calculations). The proper ordering of the $\pi\pi^*$ excitations is well reproduced, namely the excitation energy increases in going from cytosine to guanine to adenine. Moreover, the LUMO state has always a $\pi$-like character whereas the HOMO is $\pi$-like for the purines and $\sigma$-like for the pyrimidines.

Regarding the base assemblies (WC H-bond pairs and stacked configurations), the shape of the spectrum is not much altered by the $\pi$-stacking or H-bond interactions. However, hypochromicity (intensity decrease) is observed in the high energy range of the spectrum. The hypochromicity induced by $\pi$-stacking is larger than that induced by H-bonding. In the case of H-bonded basis, for light polarised perpendicular to the bases there is a blue-shift of the spectra compared to the spectra of the isolated bases. The photoabsorption cross section along this direction is mainly due to the contribution of $n\pi^*$ excitations and turns out to be orders of magnitude less intense than the spectrum for light polarised along the plane, due to $\pi\pi^*$ excitations. In the stacked case, the HOMO and LUMO states are distributed both on the purine and pyrimidine bases, whereas in the H-bonded configuration the HOMO is in the purine and the LUMO in the pyrimidine (charge transfer-type excitation). When combining both H-bonding and $\pi$-stacking, the two effects add independently, and the hypochromicity in the UV is enhanced.

Fig. 6 demonstrates some of these aspects, namely the effect of the H-bonding and $\pi$-stacking in the optical absorption. It displays the spectra for the H-bonded GC ("$GC_H$") and AT ("$AT_H$") pairs. In order to characterise the effect of the bonding, the spectra of the pairs (solid lines) is compared with the linear combination of the spectra of the isolated basis (dashed lines). The features evidenced by the figure are: (i) a small shift found for the lowest frequency peaks; (ii) the hypochromicity at high frequencies; and (iii) an overall blue-shift of the spectrum for light polarised perpendicular to the pair (not shown). In addition to the above features that originate from the individual bases, new features appear in the spectra because the purine and the pyramidine coexist in the WC arrangement. This coexistence changes the nature of the frontier orbitals: the HOMO is purine-localised, the LUMO is pyramidine-localised (bottom part of Fig. 6), and the value of the HOMO-LUMO gap is smaller than in the isolated bases. Consequently, peaks at lower energies with oscillation strengths orders of magnitude smaller than the $\pi\pi^*$ peaks, or totally dark, emerge in the spectra. These excitations, as for instances the HOMO-LUMO excitation are, consequently, of charge-transfer type.

The role of these charge-transfer excitations needs to be analysed more in detail in order to understand their impact in the excited state dynamics of DNA-based complexes (note that those states are very likely to be dark, or with very low oscillator strength for light-induced electronic excitations). In particular it is important to address which level of exchange-correlation functionals work well to describe properly this effects (see Section 6).

In the second row of Fig. 6 are shown the absorption spectra for the stacked $GC_S$ dimer (left) and for two stacked $GC_H$ stacked pairs. As in the case of hydrogen bonding, the shape of the spectrum is not strongly altered, but important differences are encountered in the oscillator strength, which turns out to be substantially reduced (hypochromism). In particular, looking at the spectrum of the two stacked $GC_S$ dimers d(GC), we find the shape of the spectrum very

Please cite this article in press as: A. Castro et al., The challenge of predicting optical properties of biomolecules: what can we learn from time-dependent density-functional theory?, C. R. Physique (2008), doi:10.1016/j.crhy.2008.09.001

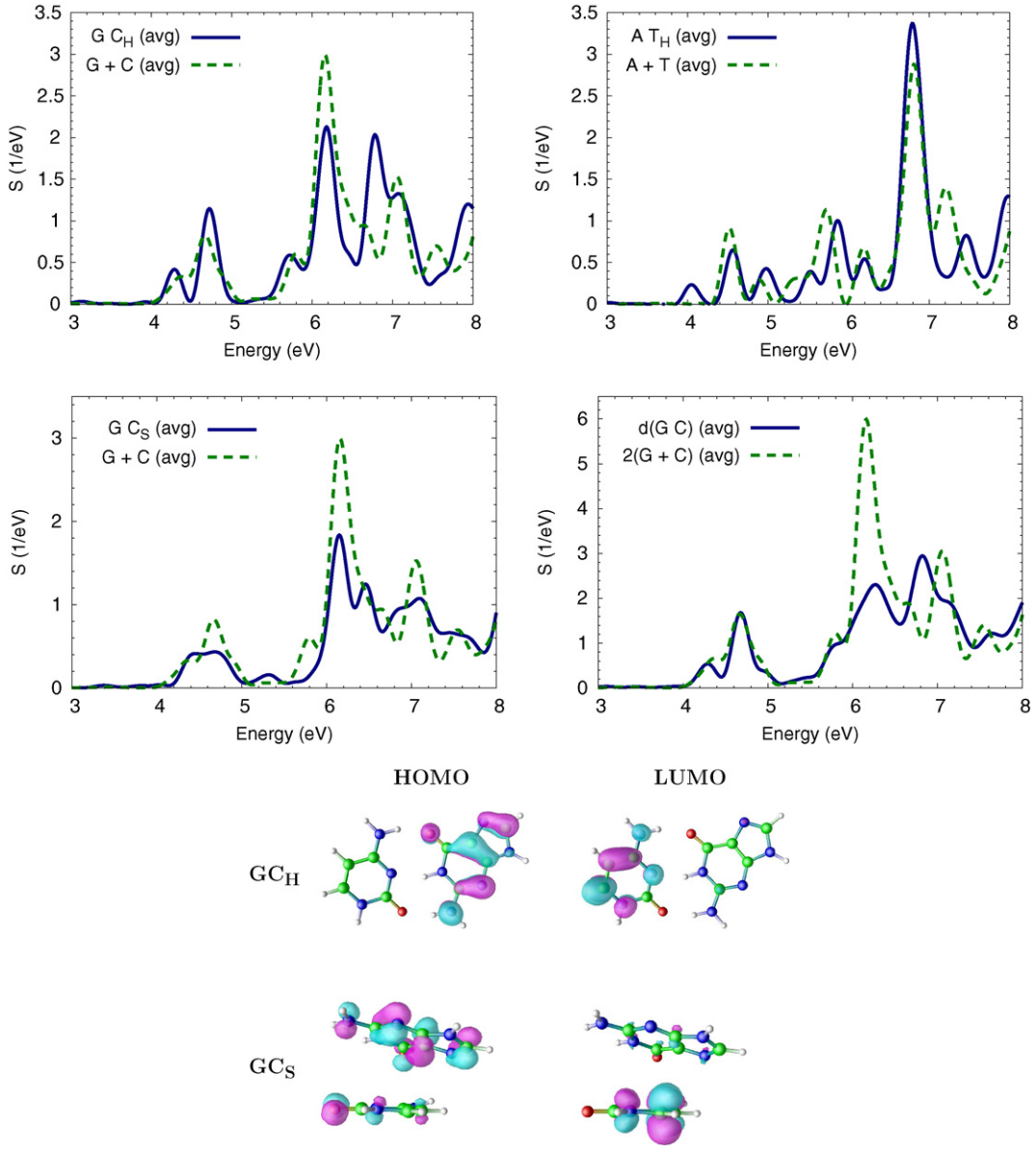


Fig. 6. Average photoabsorption cross section of the $GC_H$ and $AT_H$ base pairs (solid blue, top), and averaged spectra of stacked guanine and cytosine $GC_S$ and of two stacked WC $GC_H$ pairs d(GC) (solid blue, bottom). The linear combination of the spectra of the isolated purine and corresponding pyrimidine (G + C and A + T; dashed lines) are also shown for comparison. Below the spectra, the structures of the $GC_H$ pairs and d(GC) assembly are shown, along with the HOMO and LUMO KS wave functions.

similar to the $GC_H$ pair, but again strongly reduced in intensity because of the stacking. This feature indicates that the two kinds of base couplings seem to act separately and independently, in the sense that on does not affect the other in the optical response. The major effect of the stacking is the hypochromicity, which is very useful because the intensity change can be used to follow the melting of the secondary structure of nucleic acids when varying the temperature or environmental parameters.

Hypochromicity gives us a direct measure of the stacking interaction between bases for different systems, as for instances different DNA-like double helices, obtained modifying the base heterocycles or changing the backbone [45–47], that may be exploited for nano-electronics applications. Among these systems, particularly interesting is the expanded DNA (XDNA), obtained by Kool's group [48], where each DNA base is expanded with a benzene ring that

Please cite this article in press as: A. Castro et al., The challenge of predicting optical properties of biomolecules: what can we learn from time-dependent density-functional theory?, C. R. Physique (2008), doi:10.1016/j.crhy.2008.09.001

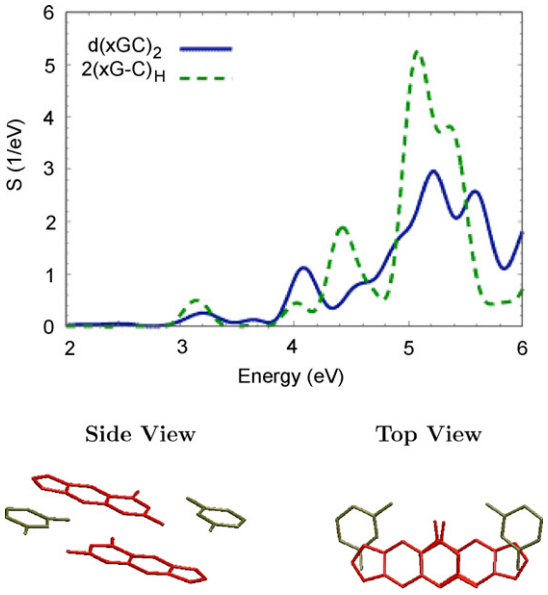


Fig. 7. Calculated dipole strength function for two stacked xG–C pairs with the expanded guanine in different strands [$d(xGC)_2$], in gas phase (solid line). The double of the absorption spectrum of the H-bonded xG–C is also shown with the green dotted line. In the bottom part of the figure the atomic structure from the top view and side view for the [$d(xGC)_2$], constructed from NMR average parameters is shown. Different bases are indicated with different colours: xG(red), C(green). Note the quite perfect overlap between the terminal part of the xG in the opposite strands.

is covalently bonded to the base and co-planar with it. Such expanded bases are able to pair with natural DNA bases by H-bonding, forming base pairs of expanded size, that stacks with each other and with natural bases, assembling helical motifs. Double helices of this kind are more stable than natural DNA, and this enhanced stability was interpreted as a consequence of enhanced stacking whether within each strand or across the strands [49]. A stacked pair of expanded guanine (xG) and cytosine (C) is sketched in Fig. 7. In Ref. [50] a detailed study of the optical properties for all the isolated expanded bases, the $xGC_H$, the $xAT_H$ and some stacked configurations is reported. TDDFT, as in the case of natural DNA bases, gives satisfactory results when compared with the available experiments [51,52] for all the benzo-fused bases, in particular for the appearance of the onset of absorption at a smaller energy (around 3.5 eV) than in any natural nucleobase: this onset peak is the novel feature induced by the benzene-base fusion. Moreover, also the more intense peaks above 4 eV are well reproduced by TDDFT calculations (see Figs. 2 and 3 in Ref. [50]). In Fig. 7 the optical spectrum for two stacked xG–C pairs with the expanded guanine in different strands [$d(xGC)_2$] is shown and is compared with the double of the absorption spectrum of the H-bonded xG–C pair. Similar effects found for natural DNA assemblies are observed also for the expanded analogues. In particular for all the studied stacked complexes the main trait is the pronounced hypochromicity, which is largest for the planar structures where the stacking interaction are mostly favoured, as in the case of $d(xGC)_2$ shown in the figure. For this case, where an enhanced interplane overlap is present, the hypochromicity is more pronounced than in natural DNA. The enhanced stacking interaction between base pairs could have consequences on the conductance and rates of electron/hole transfer, making xDNA helices very appealing for future nanoelectronics applications.

Besides optical absorption, another optical technique that is even more widely used for the characterisation of chiral biomolecules is circular dichroism. TDDFT, in its real-time propagation scheme, allows for a straightforward calculation of the rotatory power or circular dichroism spectra (see Ref. [53] for the details). The implementation and computation of circular dichroism spectra by TDDFT in real-time is in progress and will be the topic of a self-standing investigation [54], that should allow the identification of helical fingerprints in the optical characteristics, and more direct interpretation of standard post-synthesis experimental data. Just as an example, we show in Fig. 8 the calculated optical absorption, and circular dichroism spectra for an isolated adenine base (A) and a stacked dimer made of two adenines ($dA_2$) having interplane distance of 3.4 Å and a twist angle of 36°.

The absorption spectra of the isolated adenine and the dimer (top panel) have practically the same shape and the hyphocromicity induced by the stacking interaction discussed above is observed, and the excitation energies at 182,

Please cite this article in press as: A. Castro et al., The challenge of predicting optical properties of biomolecules: what can we learn from time-dependent density-functional theory?, C. R. Physique (2008), doi:10.1016/j.crhy.2008.09.001

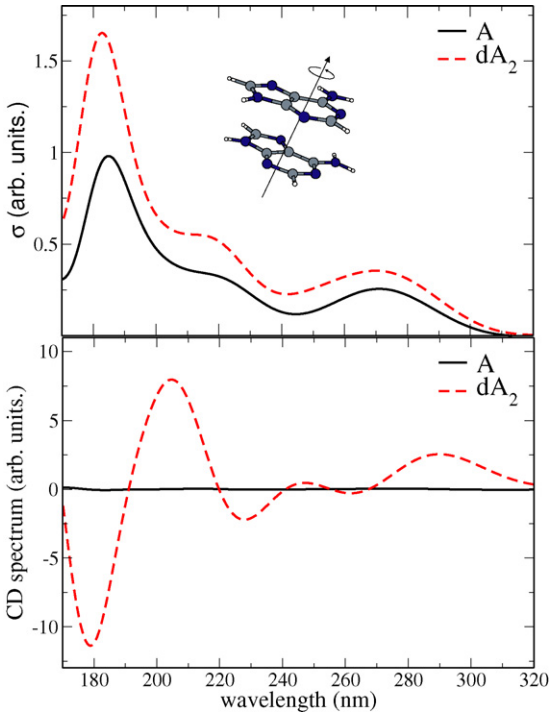


Fig. 8. Calculated dipole strength function (top) and circular dichroism (bottom) for an isolated adenine base (solid line) and for a stacked dimer of two adenines (dashed line). The structure of the stacked dimer is also shown in the insert.

215, and 270 nm (6.9, 5.76 and 4.59 eV) and the shape of the spectrum are in very good agreement with recent experiments [55]. Totally different is the circular dichroism signal: while the optical rotatory power of an isolated adenine is very small in the considered range of energies, we observe a strong signal for the dimer induced by the helical motif, with strong negative and positive bands at 180 nm and 200 nm (6.9 and 6.2 eV, respectively), in satisfactory agreement with recent experimental data where the negative and positive peaks are measured respectively at 182 nm and 194 nm [55].

## 5. Dynamics of biological molecules and TDDFT

Upon absorption of light, the associated electronic transition may trigger a subsequent nuclear dynamics: photodissociation, photo-isomerisation, etc. These relaxation processes are crucial to the understanding of many biomolecular processes, such as, e.g., the isomerisation of retinol. TDDFT is solely concerned with the electronic structure and in order to study the coupled electron-ion dynamics we need to either extend it or couple it with some flavour of molecular dynamics (MD).

Ideally, one could make use of multi-component TDDFT [56], which treats both electrons and nuclei quantum-mechanically, and on the same footing. This approach, however, is still immature and the computational resources that it would require are still out of reach. MD, on the other hand, assumes classical nuclei, which is sufficient for many purposes, although its formulation involves addressing the difficult problem of non-adiabaticity.

MD can be used in conjunction with TDDFT in various different ways, depending on the purpose and of the computational requirements of the particular system that is addressed. For example, one may perform classical, Born–Oppenheimer MD on the ground state energy surface making use of DFT, and use TDDFT to obtain the time-resolved absorption spectrum – simply performing one TDDFT calculation at sampled points in the molecular trajectory. One example of this approach is given below – applied to the azobenzene dye. This approach, however, does not address the electronic excited states (and therefore, the photon absorption processes) nor the possibility of non-adiabaticity.

In order to allow for electronic transitions, one can use, among others: Ehrenfest dynamics, and surface hopping [70,71]. In the former case, the forces on the (classical, point particle) nuclei are calculated “on the fly” by making use

Please cite this article in press as: A. Castro et al., The challenge of predicting optical properties of biomolecules: what can we learn from time-dependent density-functional theory?, C. R. Physique (2008), doi:10.1016/j.crhy.2008.09.001

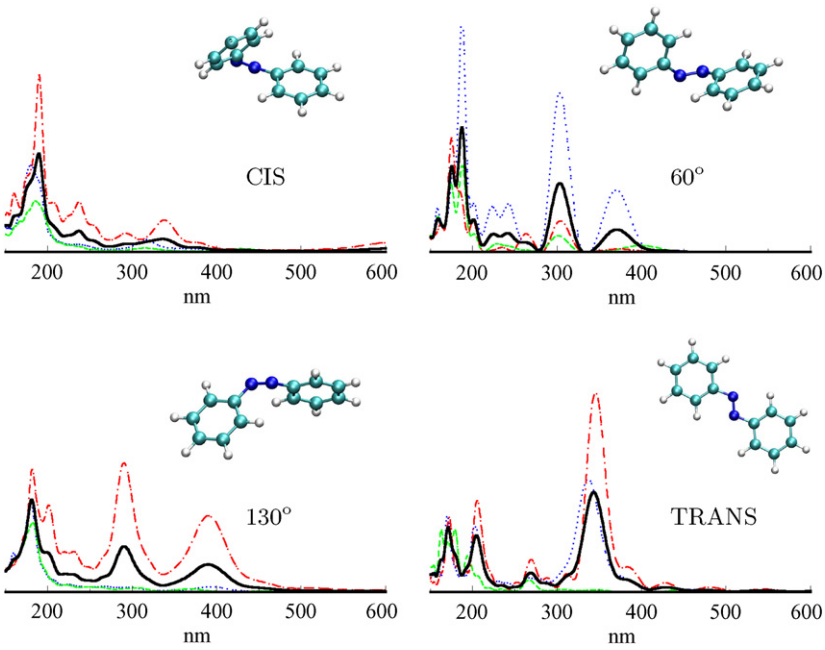


Fig. 9. Calculated photoabsorption spectra of the isolated azobenzene chromophore, at four points along an approximate isomerisation path connecting the cis and the trans conformations. The black curve represents the average absorption; the coloured lines are the decomposition of the spectra into different spatial directions, showing the anisotropy.

of the Ehrenfest theorem (i.e., the force on a nucleus is the expectation value of the partial derivative of the electronic Hamiltonian with respect to the nuclear coordinate). The electronic equations incorporate the nuclear positions as time-varying parameters, and an external, classical, electromagnetic field may also be included. In the surface-hopping scheme, one performs classical adiabatic MD on ground or excited state surfaces, and a stochastic algorithm permits to "hop" between them. We will illustrate below the TDDFT-based Ehrenfest approach. Another example, and the theoretical and computational details of our approach are given in Refs. [73,74]. We also refer the reader to the last section of this article (Section 6) for a brief discussion of the problems related to the combination of classical ion dynamics with quantum electron dynamics (for a nice review on this topic see, for example, Ref. [75]).

### *5.1. The azobenzene dye*

The azobenzene molecule is formed by two phenyl rings joined by an azo group (see Fig. 9 where it is depicted in various conformations). It undergoes very rapid (below the picosecond) cis/trans isomerisation around the N=N bond with very high efficiency [40]. This isomerisation implies an increase of 3 Å and a change in the dipole moment from 6 to 9 Debye. This property has arised great interest on azobenzene-related systems for nanoscale opto-mechanical devices. Furthermore this structural change goes together with a change in dipole moment that can be used to act as a optical-gate in, for example, nanotube-based transistors [41,42]. More relevant for the present work, in Ref. [43], Spörlein et al. have performed femtosecond time-resolved optical spectroscopy on a certain small peptide (APB), which acts as an optical trigger due to the presence of azobenzene. Their results demonstrate how the absorbance is strongly red-shifted upon cis/trans isomerisation. This pronounced spectral difference permits both a selective light-induced interconversion and easy spectroscopical differentiation. We have addressed this problem within our TDDFT formulation: Fig. 9 depicts our calculated photoabsorption spectra for four selected nuclear conformations selected along one predefined approximate isomerisation path joining the cis and trans positions. It must be noted that the peptide backbone has been only used to relax the nuclear conformations – the isomerisation path has been obtained by minimisation using a semiempirical QM/MM approach. Later the peptide backbone has been cut, and TDDFT calculations have been performed only on the azobenzene molecule. The results, nevertheless, show a redshift of most

Please cite this article in press as: A. Castro et al., The challenge of predicting optical properties of biomolecules: what can we learn from time-dependent density-functional theory?, C. R. Physique (2008), doi:10.1016/j.crhy.2008.09.001

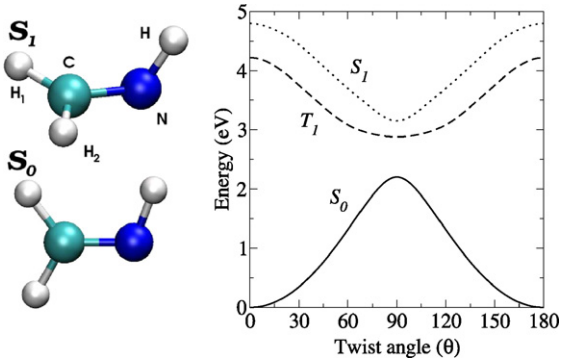


Fig. 10. Left: Geometries of the ground ($S_0$) – below – and $S_1$ – above – states of the formaldimine molecule. Right: Energy surfaces of the ground and first excited singlet and triplet states, as a function of the twist angle of the C=N bond – which is simultaneously elongated, see text.

of the spectral weight, in the same manner than the experiment. The position of the main peak does not coincide, which may be due to neglecting the influence of the peptide.

### 5.2. *Formaldimine*

Imines are those compounds of structure $RN{=}CR_2$, where R may be hydrogen or any hydrocarbyl group. Relatedly, Schiff's bases are those imines bearing a hydrocarbyl group on the nitrogen atom: $R'N{=}CR_2$ ($R'$ not equal to H). Formaldimine ($HN{=}CH_2$, see Fig. 10), also known as methanimine, is the smallest imine, and sometimes is also referred as the smallest Schiff base. In Fig. 10 we have depicted the geometries of the ground state ($S_0$) and first singlet excited state ($S_1$). The former is planar, whereas in the latter the hydrogen associated to nitrogen is rotated 90 degrees with respect to the plane of the rest of the molecule. The molecule presents a hetero double bond, C=N, which is one of the most important photoreceptors in organic chemistry: Photo-induced rotation around double bonds are processes of primary interest in Biochemistry (the paradigmatic case being the rotation of the molecular trigger of the human vision process).

Due to this relevance, formaldimine and its protonated counterpart, formaldiminium or methaniminium, has already been studied as a prototypical case-study. Bonačić–Koutecký and others [57,58,66,67] have performed multireference configuration interaction calculations of the electronic structure and geometrical conformations of the lowest singlet and triplet states. The focus was placed on the implications on photochemistry, by regarding the potential energy surfaces along possible isomerisation paths: the *cis* ↔ *trans* rearrangement may proceed via two different paths: in plane – by moving H along the $H_1H_2CN$ plane – or out of plane – by transversing the $S_1$ geometry depicted in Fig. 10. Note that in the case of formaldimine the *cis* or *trans* character of a conformation is ambiguous. Moreover, the discussed isomerisation leaves the molecule unchanged. More interesting cases in Biochemistry (e.g. the isomerisation of retinal in the vision process) also imply double bond rotations, although in these cases the product and the reactant are not identical. The out-of-plane route for the formaldimine isomerisation seemed to be favoured energetically. Moreover, the surface energy curves demonstrate the existence of a conical intersection between the first two electronic singlet states in this latter path, leading to the necessity of a truly non-adiabatic treatment.

More recently, Parrinello and others [68,69] have addressed the topic in the framework of DFT. In a former publication [68], they translated restricted open-shell Hartree–Fock (ROHF) to the Kohn–Sham formalism (restricted open-shell Kohn–Sham, ROKS), and studied the geometry of excited singlet states of several molecules, including formaldimine. They also used this technique to perform Car–Parrinello adiabatic molecular dynamics on the first excited singlet step. In the latter work [69] they extended the formalism to allow for non-adiabatic transitions via the surface-hopping algorithm [70,71]. Both works suggest the out-of-plane isomerisation.

In organic photochemistry, usually the only relevant excited states are the low lying ones. Of special relevance are the first singlet $S_1$ and the first triplet $T_1$. Since the latter is the lowest one with triplet spin symmetry, ground state DFT theory may be used to investigate it, in contrast to the $S_1$ state, which requires other approaches. However, following Frank and others [68], we may utilise Ziegler's sum method [72] and calculate the singlet excitation energy by making use only of standard DFT, in the following manner: Let us call $\Phi^{\mathrm{GS}}$ the ground state of a closed shell system such

as the formaldimine molecule, which in DFT is built from the Slater determinant of a set of Kohn–Sham orbitals: $\Phi^{\mathrm{GS}} = \mathrm{Slater}\{\psi_1\bar{\psi}_1, \ldots, \psi_n\bar{\psi}_n\}$, where the overlined orbitals are spin up. The first triplet states may be obtained by minimising a set of KS orbitals with the following fixed spin symmetry: $\Phi^{\mathrm{t}_1} = \mathrm{Slater}\{\psi_1\bar{\psi}_1, \ldots, \bar{\psi}_n\bar{\psi}_{n+1}\}$. Another of the three degenerate triplet states is obtained by using spin down for the last two orbitals. Unfortunately, the first excited singlet state cannot be obtained from a single Slater determinant. We may define the "mixed states", $\mathrm{m}_1$ and $\mathrm{m}_2$, as $\Phi^{\mathrm{m}_1} = \mathrm{Slater}\{\psi_1\bar{\psi}_1, \ldots, \psi_n\bar{\psi}_{n+1}\}$ and $\Phi^{\mathrm{m}_2} = \mathrm{Slater}\{\psi_1\bar{\psi}_1, \ldots, \bar{\psi}_n\psi_{n+1}\}$. The remaining triplet and the singlet may then be obtained by combining them:

$$\Phi^{t_3} = \frac{1}{\sqrt{2}}\left(\Phi^{m_1} - \Phi^{m_2}\right) \tag{1}$$

$$\Phi^{s} = \frac{1}{\sqrt{2}}\left(\Phi^{m_1} + \Phi^{m_2}\right) \tag{2}$$

The singlet energy may then be obtained from the energies of the $m$ and $t$ states, as in:

$$E(s) = 2E(m) - E(t) \tag{3}$$

For the $S_0$ geometrical configuration (planar, lower part of Fig. 10, this procedure yields a singlet excitation energy of 4.8 eV, in agreement with the LDA work of Ref. [68]. This scheme also allows us to obtain a minimised geometry for the $S_1$ subspace. However, we have not made a fully unrestricted seek: to alleviate the calculational burden, we have assumed the shape depicted the upper part of Fig. 10: The HCN plane is assumed to be perpendicular to the $H_1H_2CN$ plane. All geometrical parameters are then fixed to the values they have in the $S_0$ configuration, except for the C=N bond length which is then allowed to relax. The elongation of the bond in the singlet state thus obtained is 0.102 Å, in good agreement with the 0.085 Å of Ref. [68].

We then consider the rotation between the $S_0$ and $S_1$ geometries. For that purpose, we define a given path joining both geometries in configuration space: defining $\theta$ to be the twist angle around the C=N bond, the C=N bond length $l(\theta)$ is continuously elongated as $l(\theta) = \sin^2(\theta)l(0) + \cos^2(\theta)l(\pi/2)$. Along these geometries, we may sample a given number of configurations and study the excited states energies by calculating the linear response optical spectrum. We may utilise the two methods that we dispose of: linear response in the frequency domain, and time propagation. For the first singlet and triplet states energy, we may also use again previous sum rule.

The results when using Eq. (3) (i.e., still ground state DFT) are displayed in Fig. 10 (right side). The figure is in agreement with Fig. 7 in Ref. [57], where a CI method was employed. Note that for this line in configuration space we do not observe a conical intersection, but an avoided crossing. However, the surfaces do cross [58], although a different path should have been chosen to manifest it. In any case, note how the ground and excited states approach, which involves a non-negligible jump probability, and signal this isomerisation process as an intrinsically non-adiabatic one.

The photoabsorption cross sections calculated at seven points in configuration space linking the $S_0$ and $S_1$ geometries are shown in Fig. 11. It displays results obtained with two common formulations of the linear-response TDDFT equations: Casida's approach [59,60] in the frequency domain, and the real-time propagation scheme [61–65]. The red curves are the result of the scheme in the time-domain, whereas the black curves are the result for the scheme in the frequency domain (in this latter case, the lines have been broadened with a Lorentzian curve for comparison purposes). In principle, both methods are mathematically equivalent: the results, specially for the lowest excitations, are indeed very similar. The differences, whose importance increases with the excitation energy, must be assigned to the distinct numerical convergence issues arising in both methods (number of considered virtual orbitals, simulation box size, etc.), which affect the results in an inequivalent way. At full convergence, both curves should overlap.

The excitation to the first triplet configuration $T_1$ is dark, but the excitation to the first singlet $S_0$ is present in the graphs (at 4.8 eV for the geometry at $\theta = 0°$, top panel), albeit its small oscillator strength makes it difficult to see it. The insert in the top panel exposes it more clearly. The potential energy surfaces such as the one presented in Fig. 10 may also be reproduced from this figure – moreover, including, if desired, higher lying energy surfaces. The agreement for the $S_0$ state between these linear response calculations, and those presented in Fig. 10 is almost perfect.

As mentioned above, the molecular dynamics on the $S_1$ excited state have been investigated already in Ref. [68], as well as non-adiabatic dynamics [69], mixing the ground and the excited state by making use of the surface-hopping idea. Our approach to the simulation of photo-induced geometrical re-organisation is different: we make use of TDDFT to couple the ionic and electronic subsystems to a time-dependent, arbitrarily shaped, classically described, electromagnetic field. A significant laser induced population of an electronic excited state may lead to geometrical

Please cite this article in press as: A. Castro et al., The challenge of predicting optical properties of biomolecules: what can we learn from time-dependent density-functional theory?, C. R. Physique (2008), doi:10.1016/j.crhy.2008.09.001

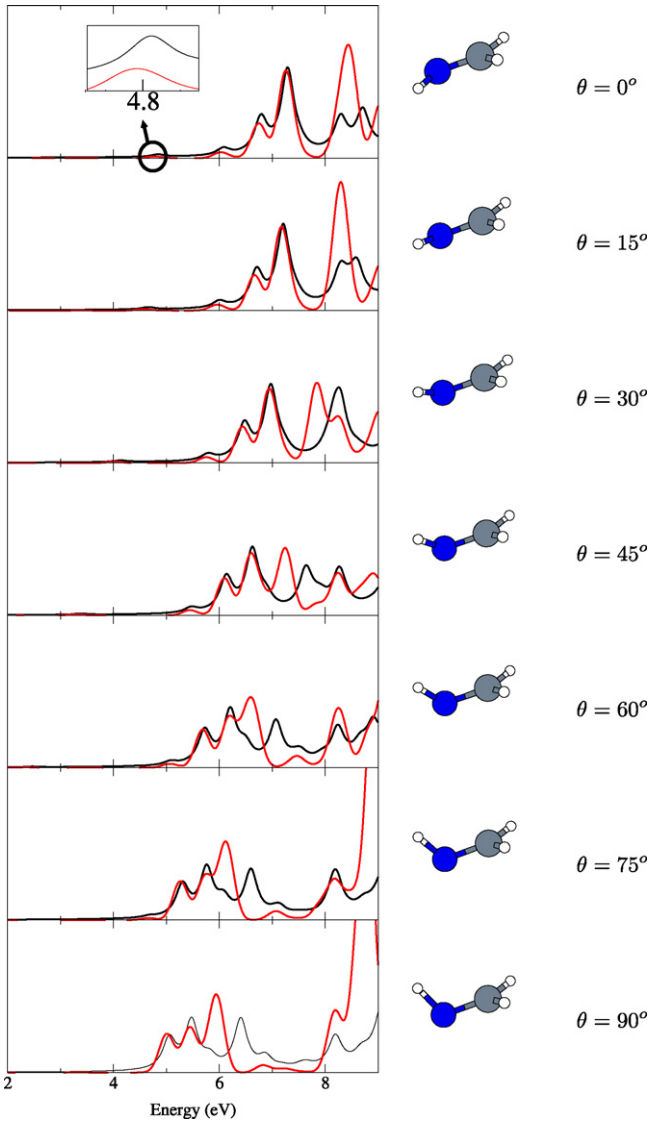


Fig. 11. Photoabsorption cross section of the formaldimine molecule, calculated at some sampled points along an isomerisation path linking the predicted $S_0$ and $S_1$ geometries (see text for details). Red: time-propagation method; Black: frequency domain line response method. The insert in the upper panel details the $S_0$ excitation, of very low oscillator strength, at 4.8 eV.

re-organisation, which means processes such as photo-fragmentation or photo-isomerisation. Some examples of this approach to photo-dissociation are described in Ref. [73]. In the present case, however, we have tried populating the $S_1$ state, which should lead to an atomic rearrangement leading to the minimum energy conformation for that state, i.e. the upper model in Fig. 10. However, we have not yet been able of observing this process. One of the explanations for this failure is the very low oscillator strength of the pursued transition, which renders difficult its population, even though we performed the simulations modelling high-intensity lasers. Another more fundamental open question is ascertaining to which extent the classical treatment of the electromagnetic fields may be suitable for these purposes.

The simulations depicted in Figs. 12 and 13 are different examples. In both cases, we have used a more traditional approach, which consists of artificially preparing the system in an excited state by populating the LUMO orbital with one electron. Thereafter, TDDFT is used to propagate the electronic state, whereas the nuclei are also propagated governed by Newton's equations of motion, according to the Ehrenfest-path methodology. In the first example (Fig. 12), the ions are initially static, and the resulting dynamics consist of an in-plane isomerisation: the hydrogen atom at-

Please cite this article in press as: A. Castro et al., The challenge of predicting optical properties of biomolecules: what can we learn from time-dependent density-functional theory?, C. R. Physique (2008), doi:10.1016/j.crhy.2008.09.001

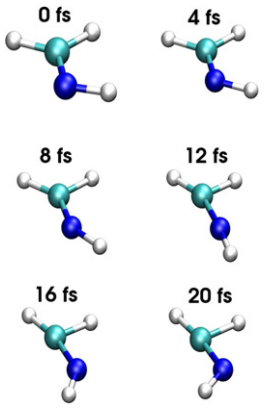


Fig. 12. Snapshots of a simulation performed on the formaldimine molecule. The system is initially prepared by putting one electron of the HOMO on the LUMO orbital. The ionic system is initially frozen.

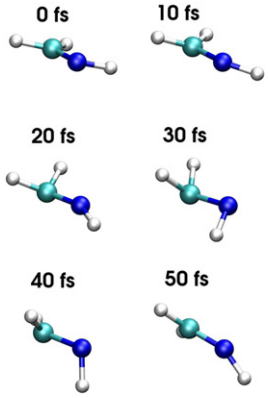


Fig. 13. Snapshots of one of the simulations performed on the formaldimine molecule. The system is initially prepared by putting one electron of the HOMO on the LUMO orbital. The ionic system is initially given a random distribution of velocities corresponding to 300 K.

tached to nitrogen pendulates from one side to the other, without leaving the original molecular plane. The movement is very rapid; the isomerisation needs only 20 fs. If the simulation is allowed to continue, the process is repeated in the same manner. In the second example (Fig. 13) the ionic system is given an initial random velocity distribution corresponding to a temperature of 300 K. The result is rather different: the molecule is rather distorted, and after an oscillation of the hydrogen atom from one molecular side to the other (which lasts only 20 fs), it goes back to its original position but following the out-of-plane route.

### *5.3. The time-dependent electron localisation function*

The real-time dynamics calculations based on TDDFT, such as the ones presented in the previous section, permit us to observe organic chemistry "in action", and in principle should allow us to see how bonds are born and die during chemical reactions, or how they are altered by the presence of an external field. The concept of "bond", however, is an elusive one, and we wish to finish this section on applications of TDDFT with an excursion to a topic that may help to gain intuition about this concept: the electron localisation function (ELF), and the time-dependent ELF (TDELF).

The concept of bond is based on that of electron pair, and was already systematised by G.N. Lewis [76] in 1916. Electrons form pairs due to their $1/2$ spin and Pauli's exclusion principle, and close "shells" – of eight electrons in many atoms due to their spherical symmetry. The preference for pairing and closing shells seemed to explain most bonding in Chemistry. This simple picture of Lewis is still in use today, and the reason is that electrons do indeed "localise" in pairs when forming molecules, and a big amount of the basic machinery of Chemistry is rather well explained with Lewis arguments. We speak of "localised" groups of electrons, either pairs of electrons shared between atoms ("bonds"), non-bonding pairs of electrons ("lone pairs"), and also larger groups – double, triple bonds –, atomic inner shells, $\pi$ electronic systems, etc.

How can one transfer these concepts to mathematical terms? It is not easy to "define" bonds from electronic densities and wave functions. In order to shed light into this problem, the concept of "electron localisation function" (ELF) was tailored by Becke and Edgecombe [77]; a concept that was later extended for time-dependent phenomena thanks to the time-dependent ELF function (TDELF) [78]. The ELF has repeatedly been used to obtain intuitive pictures of bonding properties in molecules in the ground state; the TDELF, in turn, monitored during a TDDFT-based simulation, helps to visualise time-dependent molecular processes.

We briefly recall the definitions: [77,79,80,78,81,82]

$$\eta(\mathbf{r};t) = \frac{1}{1+[C(\mathbf{r};t)/C^{\mathrm{HEG}}(\mathbf{r};t)]^2} \tag{4}$$

Please cite this article in press as: A. Castro et al., The challenge of predicting optical properties of biomolecules: what can we learn from time-dependent density-functional theory?, C. R. Physique (2008), doi:10.1016/j.crhy.2008.09.001

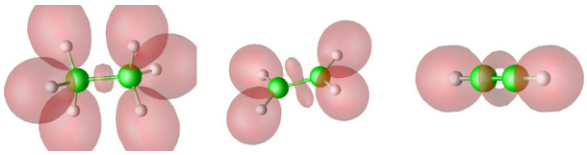

Fig. 14. ELF isosurfaces ($\eta = 0.85$) of ethane (left), ethene (center) and ethyne (right). The single bond of ethane shows as a convex ELF basin between the carbon atoms; the double bond of ethene originates two bond attractos, which in turn imply an eight-shaped ELF isosurface between the carbons), whereas the triple bond of the linear ethyne shows as a ring.

$$C(\mathbf{r};t) = \sum_{\sigma=\uparrow,\downarrow} \left\{ \tau_\sigma(\mathbf{r};t) - \frac{1}{4}\frac{[\nabla n_\sigma(\mathbf{r};t)]^2}{n_\sigma(\mathbf{r};t)} - \frac{j_\sigma^2(\mathbf{r};t)}{n_\sigma(\mathbf{r};t)} \right\} \tag{5}$$

where $\eta$ is the (TD)ELF function, $\tau_\sigma$ is the kinetic energy density, and $j_\sigma^2$ is the squared modulus of the current density. $C^{\mathrm{HEG}}(\mathbf{r};t)$ is the value of the $C$ function for a homogeneous electron gas whose density coincides with the density at point $\mathbf{r}$. This expression is valid only for one-determinantal wave functions, and therefore lends itself to be used within the context of Hartree–Fock or (TD)DFT. An exact definition, in terms of the one-reduced density matrix, can be found, for example, in the seminal Ref. [77]. We should note that the last term of Eq. (5), depending on the current, is, however, neglected in that original derivation, which assumed real-valued wave functions. That term is necessary in the time-dependent case [78].

One may then relate the topology of the ELF to the electron localisation properties of the molecules – which in turn are related to their bonding properties. The ELF takes values between 0 and 1 – high values correspond with high localisation (bonds, lone pairs), whereas low values correspond with delocalised electrons. As a scalar bounded function, it will have attractors and basins; these basins may be *core* basins (their domain contains one nucleus), bonding (located between core attractors) and non-bonding (the rest, that contain the lone-pairs of electrons). In this way, the ELF basins show us the bonds and the lone pairs of the molecules.

We plot in Fig. 14 a classical illustration of the ELF ability to mark bonds: the single, double and triple bond ethane, ethene, and ethyne, respectively. However, our main goal here is to show the TDELF in a dynamical process. We have chosen for that purpose the collision of the acetylene and oxygen molecules, which for the particular chosen initial conditions, leads to the creation of two carbon monoxide molecules (i.e. combustion).

The simulation is performed with the non-adiabatic molecular dynamics based on TDDFT described in the previous section; for this particular example we have used the simple-minded local density approximation (LDA) to the exchange and correlation functional. Some snapshots taken during the simulation are show in Fig. 15. The initial orientation and placement of the molecules is the one depicted in the first snapshot. Their relative initial velocity is $7 \times 10^{-3}$ a.u. The plot shows, besides the atomic positions (carbon in green, oxygen in red, hydrogen in white), one isosurface of the ELF ($\eta = 0.8$), which contours regions of high electron localisation. The isosurface is coloured: redder areas correspond to higher electron density, whereas whitish areas correspond to regions of almost negligible density. We have done this in order to make apparent one of the less intuitive features of the ELF: it may have large values in regions of low electronic density.

Initially, the acetylene molecule displays its characteristic toroidal ELF isosurface, typical of triple bonds. After 20 fs, the two molecules collide, and a strong link is created between the hydrogen atom of acetylene and one oxygen. The oxygen molecule is rapidly broken due to the collision; at $t = 40$ fs we can see how one oxygen atom starts moving towards the other side of the acetylene molecule, and one of the hydrogen atoms is ejected. The triple bond between the two carbon atoms is already strongly distorted; note how this is already visible in the ELF isosurface. In the next snapshots, we start to see the lone pairs characteristic of CO molecules and the remaining hydrogen atom is also ejected, carrying away one electron.

## 6. Summary and perspectives

It is clear that the use of TDDFT in the area of photochemistry has been growing in the past decade [6]. The keys for this success are clear: First of all, TDDFT is a simple theory, easy to implement, and leads to very efficient numerical implementations. Furthermore, TDDFT is quite reliable and can be used to obtain useful information: which is evident

Please cite this article in press as: A. Castro et al., The challenge of predicting optical properties of biomolecules: what can we learn from time-dependent density-functional theory?, C. R. Physique (2008), doi:10.1016/j.crhy.2008.09.001

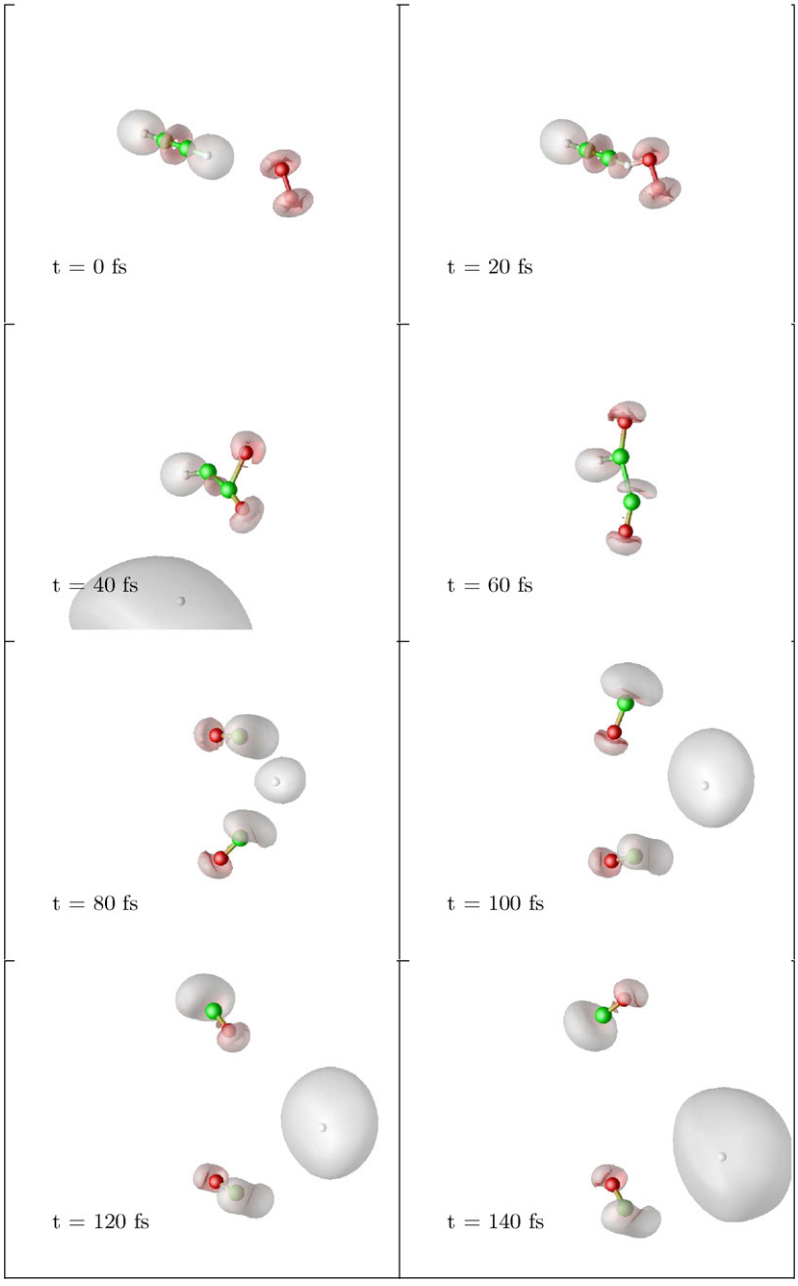


Fig. 15. Snapshots of the TDELF function (isosurface of the ELF ($\eta = 0.8$), taken during the simulation of the acetylene combustion, at the indicated times. Redder areas of the isosurface correspond to higher electron density, whereas whitish areas correspond to regions of almost negligible density.

from the examples presented in this Article. In fact, TDDFT in many cases outperforms other quantum chemical methods, especially for medium and large systems [6,11,12].

However, and in spite of its many successes, TDDFT has its shortcomings. Note that these problems are not inherent to the theory itself – which is an *exact* reformulation of time-dependent quantum-mechanics, but to the approximate functionals that are used in practical applications, or to the specific implementation of the combined electron-ion dynamics to address non-adiabatic effects in the excited-state dynamics.

One of the most important problems is related to the asymptotic behaviour of the LDA xc potential: For neutral finite systems, the exact xc potential decays as $-1/r$, whereas the LDA xc potential falls off exponentially. Note that

Please cite this article in press as: A. Castro et al., The challenge of predicting optical properties of biomolecules: what can we learn from time-dependent density-functional theory?, C. R. Physique (2008), doi:10.1016/j.crhy.2008.09.001

most of the generalised-gradient approximations (GGAs), or even the newest meta-GGAs have asymptotic behaviours similar to the LDA. This problem gains particular relevance when calculating ionisation yields (the ionisation potential calculated with the ALDA is always too small), in situations where the electrons are pushed to regions far away from the nuclei (e.g., by a strong laser) and feel the incorrect tail of the potential, or in excitations that involve Rydberg states. There are several ways to correct this problem, either by directly modelling the xc potential [83], or by using orbital functionals with the right asymptotic behaviour, like the exact exchange [84] or the self-interaction corrected [85] functionals. Along those lines it is important to mention that present local and semilocal functionals fail dramatically in describing dispersion forces (e.g., in Van der Waals complexes). At present the impact of those failures in the optical spectra of biomolecules has not been discussed in detail, and most of the cure-schemes address the problem for ground-state calculations either as a post-DFT correction [86,87], or by the use of TDDFT in the adiabatic connection/fluctuation-dissipation scheme [88,89]. Clearly there is a lot of work to be done in this context to describe the role of dispersion forces in the combined excited-state dynamics of complex biomolecules (for example to describe light-induced proton transfer and H-bond breaking/formation).

Another noteworthy problem is the absence of true multiple excitations in the TDDFT response functions. This is due to the use of the adiabatic approximation in the construction of time-dependent xc functionals. There have been some attempts at the construction of functionals including memory effects [90–96] or by including the effect of doubles excitations perturbatively [97,98].

Next, we would like to refer to charge-transfer excitations. TDDFT often predicts charge-transfer states of substantially lower energy and below optical states [99]. This is further complicated by the mismatch between the ionisation potentials of the donor and acceptor parts of the molecule, due to the absence of a derivative discontinuity in the common functionals [100]. Thus, charge-transfer excitations are severely underestimated, sometimes by as much as 1 eV. Several correction schemes have been proposed [101] for this problem. However there is not yet a good functional incorporating those processes both at the static as well as at the dynamical level. Thus, the dynamics of many biological processes that are mediated by that type of intermediate states, may not be properly accounted for by present TDDFT implementations. (Kernels based on many-body perturbation theory, as the ones derived to describe the optical properties of solids [12] could account for those excitations. However, it is still not known to which degree of accuracy.)

However, perhaps the largest failure of TDDFT is in the calculations of the optical spectra of solids [102,12]. In fact, the lack of a long-range component of the xc kernel leads to TDDFT spectra of very poor quality, only marginally different from simple RPA calculations. Again, several possible alternatives to correct this problem have been proposed, from orbital functionals that include this long-range component [103–107], to empirical correction terms to the xc kernel [108–110]. Those functionals might have implications in the description of multiple excitations, charge-transfer processes and photo-induced molecular dissociation.

Another important aspect of the specific examples discussed in this article is related to the fact that electron dynamics are usually determined quantum mechanically but the nuclear motion is treated within the framework of classical mechanics. Despite a large difference in the general time scales of electronic and nuclear motions, electronic wavepackets quite often couple with the dynamics of nuclear motion. The proper incorporation of the electronic response is crucial for describing a host of dynamical processes, including laser-induced chemistry, dynamics at metal or semiconductor surfaces, and electron transfer in molecular, biological, interfacial, or electrochemical systems (in particular it is crucial also for describing light-induced processes in biomolecules, and many other photochemical reactions). The two most widely used approaches to account for non-adiabatic effects are the surface-hopping method and the Ehrenfest method implemented here. The surface-hopping approach extends the Born–Oppenheimer framework to the non-adiabatic regime by allowing stochastic electronic transitions subject to a time- and momenta-dependent hopping probability. On the other hand Ehrenfest successfully adds some non-adiabatic features to molecular dynamics but it is rather incomplete. This approximation can fail either when the nuclei have to be treated as quantum particles (e.g. tunnelling) or when the nuclei respond to the microscopic fluctuations in the electron charge density (heating) not reproducing the correct thermal equilibrium between electrons and nuclei (which constitutes a fundamental failure when simulating the vibrational relaxation of biomolecules in solution). However there have been some proposals in the literature to include some of those effects in a modified Ehrenfest scheme [111,112] or beyond it (see, e.g. Ref. [113]).

On a more practical level, the possibility of simulating dynamics on electronic excited states requires the capability of computing forces on those states. On the electronic ground state, the computation of the force is a trivial task within

Please cite this article in press as: A. Castro et al., The challenge of predicting optical properties of biomolecules: what can we learn from time-dependent density-functional theory?, C. R. Physique (2008), doi:10.1016/j.crhy.2008.09.001

the DFT formalism because the force on an ion is an explicit functional of the ground state density (the Hellman–Feynman expression). In the Ehrenfest dynamics approach, the same expression can be used – the forces are again trivially dependent on the time-dependent density. However, if we attempt to use the same idea to perform dynamics on a given "pure" excited state, we are confronted with the problem of obtaining the corresponding excited state density – not at all a trivial task. Fortunately, one can use linear-response TDDFT in order to obtain suitable expressions (see. e.g. Refs. [114] and [115]).

In conclusion, TDDFT has become a standard tool to calculate excitation energies, and is by now incorporated in all of the major quantum-chemistry codes. There are many examples of successful applications of this theory in the literature, and its usefulness for the study of large, complex systems is unique. Clearly, there are some cases where TDDFT does not perform well. However, in our opinion, we should not dismiss these problems as failures of TDDFT, but as a challenge to the next generation of "density-functionalists", in their quest for better approximations to the elusive xc potential.

## Acknowledgements

We acknowledge the fruitful collaboration with X. López, Y. Pouillon, X. Andrade, S. Botti, M. Gruning, R. Di Felice, C. Attacalite, A. Marini, L. Wirtz, J.M. García-Lastra, F. Nogueira, M. Oliveira, F. Lorenzen, C. Rozzi, Steen B. Nielsen, and E.K.U. Gross in many parts of the work presented here. We benefited from discussions with R. Bitl, E. Molinari, and S.G. Louie. The development of this project benefited from many informal discussions with the NANOQUANTA/ETSF members as well as with the Editors and contributors to the TDDFT book [6], the outcome of the series of schools and workshops organised by some of the authors on "Time-Dependent Density-Functional Theory: Prospects and Applications", held in Benasque Spain since 2004 (see http://nano-bio.ehu.es).

We acknowledge funding by the Deutsche Forschungsgemeinschaft through SPP 1093 and SFB 658, Spanish MEC (FIS2007-65702-C02-01) and Grupos Consolidados UPV/EHU of the Basque Country Government (2007), by the European Community through NoE Nanoquanta (NMP4-CT-2004-500198), SANES (NMP4-CT-2006-017310), ANR (Project NT0S-3_43900), DNA-NANODEVICES (IST-2006-029192) and NANO-ERA Chemistry projects, UPV/EHU (SGIker Arina). MALM acknowledges partial support by the Portuguese FCT through the project PTDC/FIS/73578/2006. The authors thankfully acknowledge the computer resources provided by the Barcelona Supercomputing Center, the Basque Country University UPV/EHU (SGIker Arina) and the Laboratório de Computação Avançada of the University of Coimbra, CPU time from CINECA through INFM-CNR.

## References

[1] P.N. Prasad, Introduction to Biophotonics, John Wiley & Sons, Hoboken, 2003.
[2] K. Bacon, Photosynthesis. Photobiochemistry and Photobiophysics, Springer, Berlin, 1999.
[3] C. Musio (Ed.), Vision: The Approach of Biophysics and Neurosciences, World Scientific, Singapore, 2001.
[4] O. Shimomura, Biolumnescence: Chemical Principles and Methods, World Scientific, Singapore, 2006.
[5] O. Shoseyov, I. Levy (Eds.), NanoBioTechnology: BioInspired Devices and Materials of the Future, Humana Press, 2007.
[6] M.A.L. Marques, C. Ullrich, F. Nogueira, A. Rubio, E.K.U. Gross (Eds.), Time-Dependent Density-Functional Theory, Lecture Notes in Physics, vol. 706, Springer-Verlag, Berlin, 2006.
[7] M.A.L. Marques, A. Castro, G.F. Bertsch, A. Rubio, Comput. Phys. Commun. 151 (2003) 60.
[8] A. Castro, H. Appel, M. Oliveira, C.A. Rozzi, X. Andrade, F. Lorenzen, E.K.U. Gross, M.A.L. Marques, A. Rubio, Phys. Status Solidi B 243 (2006) 2465.
[9] E. Runge, E.K.U. Gross, Phys. Rev. Lett. 52 (1984) 997.
[10] E.K.U. Gross, W. Kohn, Adv. Quantum. Chem. 21 (1990) 255.
[11] M.A.L. Marques, E.K.U. Gross, Annu. Rev. Phys. Chem. 55 (2004) 427.
[12] G. Onida, L. Reinig, A. Rubio, Rev. Mod. Phys. 74 (2002) 601.
[13] See, for example, J. Livet, et al., Nature 450 (2007) 56.
[14] S. Takeda, N. Kamiya, Teruyuki Nagamune, Biotechnology Lett. 26 (2004) 121.
[15] T.M.H. Creemers, A.J. Lock, V. Subramaniam, T.M. Jovin, S. Völker, Proc. Natl. Acad. Sci. USA 97 (2000) 2974; T.M.H. Creemers, A.J. Lock, V. Subramaniam, T.M. Jovin, S. Völker, Nature Struct. Biol. 6 (1999) 557.
[16] S.B. Nielsen, A. Lapierre, J.U. Andersen, U.V. Pedersen, S. Tomita, L.H. Andersen, Phys. Rev. Lett. 87 (2001) 228102.
[17] M.A.L. Marques, X. López, D. Varsano, A. Castro, A. Rubio, Phys. Rev. Lett. 90 (2003) 258101.
[18] B.R. Brooks, R.E. Bruccoleri, B.D. Olafson, D.J. States, S. Swaminathan, M. Karplus, J. Comput. Chem. 2 (1983) 187.
[19] M.J. Field, P.A. Bash, M. Karplus, J. Comput. Chem. 11 (1990) 700.
[20] J. Gao, in: K.B. Lipkowitz, D.B. Boyd (Eds.), Reviews in Computational Chemistry, vol. 7, Wiley VCH, New York, 1995, p. 119.

Please cite this article in press as: A. Castro et al., The challenge of predicting optical properties of biomolecules: what can we learn from time-dependent density-functional theory?, C. R. Physique (2008), doi:10.1016/j.crhy.2008.09.001

[21] M.J.S. Dewar, E. Zoebisch, E.F. Healy, J.J.P. Stewart, J. Am. Chem. Soc. 107 (1995) 3902.
[22] R. Wachter, B. King, R. Heim, K. Kallio, R. Tsien, S. Boxer, S. Remington, Biochemistry 36 (1997) 36.
[23] B.G. Bublitz, B. King, S. Boxer, J. Am. Chem. Soc. 120 (1998) 9370.
[24] M. Zimmer, Chem. Rev. 102 (2002) 759, and references therein.
[25] M. Chattoraj, B. King, G. Bublitz, S. Boxer, Proc. Natl. Acad. Sci. USA 93 (1996) 8362.
[26] X. López, M.A.L. Marques, A. Castro, A. Rubio, J. Am. Chem. Soc. 127 (2005) 12329.
[27] M.A.L. Marques, X. Löpez, A. Castro, A. Rubio, in press.
[28] K. Kadish, K.M. Smith, R. Guilard (Eds.), The Porphyrin Handbook, Academic Press, London, 1999.
[29] M. Gouterman, in: D. Dolphin (Ed.), The Porphyrins, vol. 3, Academic Press, New York, 1973.
[30] F. Sottile, C. Hogan, M. Palummo, A. Rubio, in preparation.
[31] D. Varsano, R. Di Felice, M.A.L. Marques, A. Rubio, J. Phys. Chem. B 110 (2006) 7129.
[32] M. Daniels, in: S.Y. Yang (Ed.), Photochemistry and Photobiology of Nucleic Acids, Academic Press, New York, 1976, p. 23.
[33] C.E.C. Hernández, B. Cohen, P.M. Hare, B. Kohler, Chem. Rev. 104 (2004) 1977.
[34] D. Porath, G. Cuniberti, R.D. Felice, in: G. Schuster (Ed.), Topics in Current Chemistry, Springer-Verlag, Heidelberg, 2004, p. 183.
[35] M. Di Ventra, M. Zwolak, in: H.S. Nalwa (Ed.), Encyclopedia of Nanoscience and Nanotechnology and Handbook of Nanostructured Biomaterials and their Application in Nanotechnology, APS, College Park, MD, 2004, p. 475.
[36] R.G. Endres, D. Cox, R. Singh, Rev. Mod. Phys. 76 (2004) 195.
[37] H. Coehn, C. Nogues, R. Naaman, D. Porath, Proc. Natl. Acad. Sci. USA 102 (2005) 11589.
[38] R. Di Felice, A. Calzolari, E. Molinari, A. Garbesi, Phys. Rev. B 65 (2002) 045104.
[39] R. Di Felice, A. Calzolari, in: E.B. Starikov, S. Tanaka, J.P. Lewis (Eds.), Modern Methods for Theoretical Physical Chemistry of Biopolymers, Elsevier, Amsterdam, 2005.
[40] T. Nägele, R. Hoche, W. Zinth, J. Wachtveitl, Chem. Phys. Lett. 272 (1997) 489.
[41] J.M. Simmons, V.E. Campbell, T.J. Mark, F. Léonard, P. Gopalan, M.A. Eriksson, Phys. Rev. Lett. 98 (2007) 086802.
[42] J.M. García-Lastra, K. Thygesen, A. Rubio, Phys. Rev. Lett. 101 (2008) 13302.
[43] S. Spörlein, H. Carstens, H. Satzger, C. Renner, R. Behrendt, L. Moroder, P. Tavan, W. Zinth, J. Wachtveitl, Proc. Natl. Acad. Sci. USA 99 (2002) 7998.
[44] J.H. Watson, F.H. Crick, Nature 171 (1953) 737.
[45] A.A. Henry, F.E. Romesbergi, Curr. Opin. Chem. Biol. 7 (2003) 727.
[46] A.T. Krueger, H. Lu, A.H. Lee, E.T. Kool, Acc. Chem. Res. 40 (2007) 141.
[47] I. Hirao, Curr. Opin. Chem. Biol. 10 (2006) 622.
[48] J. Gao, H. Liu, E.T. Kool, Angew. Chem. Int. Ed. 44 (2005) 3118.
[49] H. Liu, J. Gao, S.R. Lynch, E.T. Kool, Science 302 (2003) 868.
[50] D. Varsano, A. Garbesi, R. Di Felice, J. Phys. Chem. B 111 (2007) 14012.
[51] H. Liu, J. Gao, L. Maynard, Y.D. Saito, E.T. Kool, J. Am. Chem. Soc. 126 (2004) 1102.
[52] H. Liu, J. Gao, E.T. Kool, J. Org. Chem. 70 (2005) 639.
[53] K. Yabana, G.F. Bertsch, Phys. Rev. A 60 (1999) 1271.
[54] D. Varsano, A. Castro, M.A.L. Marques, R. Di Felice, A. Rubio, in preparation.
[55] U. Kadhane, A.I.S. Holm, S.V. Hoffmann, S.B. Nielsen, Phys. Rev. E 77 (2008) 021901.
[56] T. Kreibich, E.K.U. Gross, Phys. Rev. Lett. 86 (2001) 2984.
[57] V. Bonačić-Koutecký, M. Persico, J. Am. Chem. Soc. 105 (1983) 3388.
[58] V. Bonačić-Koutecký, J. Köhler, J. Michl, Chem. Phys. Lett. 104 (1984) 440.
[59] M.E. Casida, in: D.P. Chong (Ed.), Recent Advances in Density Functional Methods, Part I, World Scientific, Singapore, 1995, p. 155.
[60] M. Casida, in: J. Seminario (Ed.), Recent Developments and Applications in Density Functional Theory, Elsevier, Amsterdam, 1996, p. 391.
[61] K. Yabana, G.F. Bertsch, Phys. Rev. B 54 (1996) 4484.
[62] K. Yabana, G.F. Bertsch, Z. Phys. D 42 (1997) 219.
[63] K. Yabana, G.F. Bertsch, Phys. Rev. A 58 (1999) 2604.
[64] K. Yabana, G.F. Bertsch, Phys. Rev. A 60 (1999) 3809.
[65] M.A.L. Marques, A. Castro, A. Rubio, J. Chem. Phys. 115 (2001) 3006.
[66] V. Bonačić-Koutecký, J. Michl, Theor. Chim. Acta 68 (1985) 45.
[67] V. Bonačić-Koutecký, K. Schöffel, J. Michl, Theor. Chim. Acta 72 (1987) 459.
[68] I. Frank, J. Hütter, D. Marx, M. Parrinello, J. Chem. Phys. 108 (1998) 4060.
[69] N.L. Doltsinis, D. Marx, Phys. Rev. Lett. 88 (2002) 166402.
[70] J.C. Tully, R.K. Preston, J. Chem. Phys. 55 (1971) 562.
[71] J.C. Tully, J. Chem. Phys. 93 (1990) 1061.
[72] T. Ziegler, A. Rauk, E.J. Baerends, Theor. Chim. Acta 43 (1977) 261.
[73] A. Castro, M.A.L. Marques, J.A. Alonso, G.F. Bertsch, A. Rubio, Eur. Phys. J. D 28 (2004) 211.
[74] A. Castro, A first-principles time-dependent density functional theory scheme for the computation of the electromagnetic response of nanostructures, PhD. Thesis, University of Valladolid, 2004. The thesis can be downloaded from http://nano-bio.ehu.es/files/acastro_phd.pdf.
[75] A.P. Horsfield, D.R. Bowler, A.J. Fisher, T.N. Todorov, C.G. Sanchez, J. Phys. Cond. Matt. 16 (2004) 8521.
[76] G.N. Lewis, J. Am. Chem. Soc. 38 (1916) 762.
[77] A.D. Becke, K.E. Edgecombe, J. Chem. Phys. 92 (1990) 5397.
[78] T. Burnus, M.A.L. Marques, E.K.U. Gross, Phys. Rev. A 71 (2005) 010501.

Please cite this article in press as: A. Castro et al., The challenge of predicting optical properties of biomolecules: what can we learn from time-dependent density-functional theory?, C. R. Physique (2008), doi:10.1016/j.crhy.2008.09.001

[79] R.F.W. Bader, S. Johnson, T.-H. Tang, P.L.A. Popelier, J. Phys. Chem. 100 (1996) 15398.
[80] J.F. Dobson, J. Chem. Phys. 98 (1993) 8870.
[81] B. Silvi, A. Savin, Nature 371 (1994) 683.
[82] A. Savin, R. Nesper, S. Wengert, T.F. Fässler, Angew. Chem. Int. Ed. Engl. 36 (1997) 1808.
[83] R. van Leeuwen, E.J. Baerends, Phys. Rev. B 49 (1994) 2421.
[84] F. Della Sala, Andreas Grling, Int. J. Quantum Chem. 91 (2003) 131.
[85] J.P. Perdew, A. Zunger, Phys. Rev. B 23 (1981) 5408.
[86] E. Hult, Y. Andersson, B.I. Lundqvist, Phys. Rev. Lett. 77 (1996) 202.
[87] H. Rydberg, M. Dion, N. Jacobson, E. Schröder, P. Hyldgaard, S.I. Simak, D.C. Langreth, B.I. Lundqvist, Phys. Rev. Lett. 91 (2003) 126402.
[88] W. Kohn, Y. Meir, D.E. Makarov, Phys. Rev. Lett. 80 (1998) 4153.
[89] J.F. Dobson, A. White, A. Rubio, Phys. Rev. Lett. 96 (2006) 073201.
[90] E. Orestes, K. Capelle, J. Chem. Phys. 127 (2007) 124101.
[91] G. Vignale, W. Kohn, Phys. Rev. Lett. 77 (1996) 2037.
[92] M.J. Bünner, E.K.U. Gross, Phys. Rev. Lett. 79 (1997) 1905.
[93] G. Vignale, C.A. Ullrich, S. Conti, Phys. Rev. Lett. 79 (1997) 4878.
[94] C.A. Ullrich, G. Vignale, Phys. Rev. B 65 (2002) 245102;
C.A. Ullrich, G. Vignale, Phys. Rev. B 70 (2004) 239903(E).
[95] Y. Kurzweil, R. Baer, J. Chem. Phys. 121 (2004) 8731.
[96] I.V. Tokatly, Phys. Rev. B 71 (2005) 165104;
I.V. Tokatly, Phys. Rev. B 71 (2005) 165105.
[97] N. Maitra, F. Zhang, R. Cave, J. Chem. Phys. 120 (2004) 5932.
[98] M. Casida, J. Chem. Phys. 122 (2004) 054111.
[99] A. Dreuw, J.L. Weisman, M. Head-Gordon, J. Chem. Phys. 119 (2003) 2943.
[100] D.J. Tozer, J. Chem. Phys. 119 (2003) 12697.
[101] D.J. Tozer, M. Head-Gordon, J. Am. Chem. Soc. 126 (2004) 4007.
[102] S. Botti, A. Schindlmayr, R. Del Sole, L. Reining, Rep. Prog. Phys. 70 (2007) 357.
[103] E.K.U. Gross, J. Dobson, M. Petersilka, in: R.F. Nalewajski (Ed.), Density Functional Theory II, in: Topics in Current Chemistry, vol. 18, Springer, Berlin, 1996.
[104] A. Görling, Phys. Rev. A 55 (1997) 2630.
[105] A. Görling, Phys. Rev. A 57 (1998) 3433.
[106] A. Görling, Int. J. Quantum Chem. 69 (1998) 265.
[107] Y.H. Kim, A. Görling, Phys. Rev. B 66 (2002) 035114.
[108] S. Botti, A. Fourreau, F. Nguyen, Y.-O. Renault, F. Sottile, L. Reining, Phys. Rev. B 72 (2005) 125203.
[109] S. Botti, F. Sottile, N. Vast, V. Olevano, L. Reining, H.-C. Weissker, A. Rubio, G. Onida, R. Del Sole, R.W. Godby, Phys. Rev. B 69 (2004) 155112.
[110] L. Reining, V. Olevano, A. Rubio, G. Onida, Phys. Rev. Lett. 88 (2002) 066404.
[111] A. Bastida, C. Cruz, J. Zúñiga, A. Requena, B. Miguel, J. Chem. Phys. 126 (2007) 014503.
[112] K. Takatsuka, J. Phys. Chem. A 111 (2007) 10196.
[113] A.P. Horsfield, D.R. Bowler, H. Ness, C.G. Sánchez, T.N. Todorov, A.J. Fisher, Rep. Prog. Phys. 69 (2006) 1195.
[114] F. Furche, R. Ahlrichs, J. Chem. Phys. 117 (2002) 7433.
[115] I. Tavernelli, U.F. Röhrig, U. Rothlisberger, Mol. Phys. 103 (2005) 963.

Please cite this article in press as: A. Castro et al., The challenge of predicting optical properties of biomolecules: what can we learn from time-dependent density-functional theory?, C. R. Physique (2008), doi:10.1016/j.crhy.2008.09.001